

See discussions, stats, and author profiles for this publication at: <https://www.researchgate.net/publication/7677055>

Impact of Vegetation on Sedimentary Organic Matter Composition and Polycyclic Aromatic Hydrocarbon Attenuation

ARTICLE *in* ENVIRONMENTAL SCIENCE AND TECHNOLOGY · AUGUST 2005

Impact Factor: 5.33 · DOI: 10.1021/es048028o · Source: PubMed

CITATIONS

25

READS

15

3 AUTHORS, INCLUDING:



Damian Shea

North Carolina State University

84 PUBLICATIONS 2,064 CITATIONS

SEE PROFILE



Elizabeth Guthrie Nichols

North Carolina State University

17 PUBLICATIONS 73 CITATIONS

SEE PROFILE

Impact of Vegetation on Sedimentary Organic Matter Composition and Polycyclic Aromatic Hydrocarbon Attenuation

SAMUEL T. GREGORY,[†]
DAMIAN SHEA,[†] AND
ELIZABETH GUTHRIE-NICHOLS*,^{†,‡}

Department of Environmental and Molecular Toxicology, and
Environmental Technology Program, North Carolina State
University, Box 8006, Raleigh, North Carolina 27695

Results from natural and engineered phytoremediation systems provide strong evidence that vegetated soils mitigate polycyclic aromatic hydrocarbon (PAH) contamination. However, the mechanisms by which PAH mitigation occurs and the impact of plant organic matter on PAH attenuation remain unclear. This study assessed the impact of plant organic matter on PAH attenuation in labile and refractory sediments fractions from a petroleum distillate waste pit that has naturally revegetated. Samples were collected in distinct zones of barren and vegetated areas to assess changes to organic matter composition and PAH content as vegetation colonized and became established in the waste pit. Sediments were fractionated into bulk sediment and humin fractions and analyzed for organic matter composition by isotope ratio mass spectrometry ($\delta^{13}\text{C}$), ^{13}C nuclear magnetic resonance (^{13}C NMR), $\Delta^{14}\text{C}$ AMS (accelerator mass spectrometry), and percent organic carbon (%TOC). Gas chromatography mass spectrometry (GC/MS) of lipid extracts of SOM fractions provided data for PAH distribution histograms, compound weathering ratios, and alkylated and nonalkylated PAH concentrations. Inputs of biogenic plant carbon, PAH weathering, and declines in PAH concentrations are most evident for vegetated SOM fractions, particularly humin fractions. Sequestered PAH metabolites were also observed in vegetated humin. These results show that plant organic matter does impact PAH attenuation in both labile and refractory fractions of petroleum distillate waste.

Introduction

The growing interest in applications of phytotechnologies to treat polycyclic aromatic hydrocarbon (PAH) contamination necessitates an improved understanding of how plant organic matter may impact the bioaccessibility of PAHs in soil/sediment organic matter (SOM) over time (1). Plants are a major source of organic matter to SOM (2) and can alter SOM composition by physical, biological, and chemical processes (3). Plants stimulate microbial activity that rapidly mineralizes labile plant materials while more resistant plant fractions transform slowly to form humic materials (2, 4–6).

Only a small percentage (20–30%) of recognizable plant organic matter remains over time in SOM (4).

The rhizosphere is a complex matrix; quantification of specific mechanisms for PAH transformation or stabilization is difficult (7). Several studies have shown that plant exudates enhance PAH degradation by invigorating microbial activity and abundance (8–10). Plant exudates, such as organic acids, also play a critical role in plant physiology and the formation and stability of humic materials (11–13). Organic acids can dissociate aggregate humic materials into smaller structures stabilized by hydrogen bonding (13–15) that can contribute to PAH sorption (12, 16–18) or PAH degradation by microbes (19).

Root exudates, such as phenolic monomers and oxidative enzymes, can also polymerize with humic materials to form larger, covalently linked aggregates (4, 18, 20) that are resistant to organic acid dissociation (21). These stable aggregate structures are conducive to sequestration of organic carbon and the binding of organic contaminants including PAHs (6, 12, 16–18). Recent studies have noted the “accumulation” or increased concentrations of PAHs and weathered 2,2-bis(*p*-chlorophenyl)-1,1-dichloroethylene (*p,p'*-DDE) in rhizosphere soil versus nonvegetated soil (9, 22, 23).

In SOM, the removal of higher molecular weight PAHs is primarily dependent on microbial transformation. However, recent studies of carbon sequestration in soils noted that increased plant exudation appeared to reduce microbial dependence on older SOM as a carbon source and retarded the mineralization of older, persistent SOM (24–26). Redirection of microbial degradation away from older SOM to fresh rhizodeposition could retard microbial-mediated liberation and transformation of PAHs.

Thus, plant organic matter may impact PAH bioaccessibility by two mechanisms. First, the rhizosphere may improve PAH bioaccessibility by destabilizing SOM via microbial degradation, organic acids, and chelating agents and liberate PAH for transformation (9, 27, 28). Alternatively, the rhizosphere may alter carbon composition and provide new carbon matrixes that further sorb and bind PAHs in biogenic SOM, thus reducing PAH bioaccessibility (6, 12, 20). Given the complexity of soil/sediment dynamics, these mechanisms may occur simultaneously.

We investigated the validity of these two mechanisms by assessing changes to SOM composition in relation to diagnostic indices of PAH attenuation for vegetated and barren sediments collected from a pit of petroleum distillate waste. The waste pit has naturally revegetated over the last 40 years and is subject to periodic tidal influx from an estuary. Although physical disturbance of SOM by plant roots can impact processes such as volatilization and leaching for some lighter PAHs (29), the unique site characteristics (age, petroleum distillate waste material, tidal fluxes) suggest that sorption dynamics between organic matter and heavier PAHs will dominate PAH dissolution and transformation (28).

If plant organic matter improves PAH bioaccessibility and ultimately PAH transformation, then diagnostic indices (PAH histograms, PAH concentrations, and compound ratios) would reflect PAH transformation by (a) statistically significant declines in PAH concentrations, (b) weathered distribution patterns in PAH histograms, and (c) weathered PAH compound ratios. If plant organic matter retards PAH bioaccessibility, then declines in PAH concentrations and weathered diagnostic indices would not be observed. PAH concentrations, distribution patterns (histograms), and compound ratios were determined by gas chromatography mass spectrometry (GC/MS) with select ion mode (SIM)

* Corresponding author phone: 919 513 4832; fax: 919 515-6193; e-mail: Elizabeth_Nichols@ncsu.edu.

[†] Department of Environmental and Molecular Toxicology.

[‡] Environmental Technology Program.

TABLE 1. Inventory of 42 Alkylated and Non-alkylated PAHs

| analyte | abbrev | no. of rings | analyte | abbrev | no. of rings |
|------------------------------|--------|--------------|-------------------------------------|--------|--------------|
| naphthalene ^a | N0 | 2 | fluoranthene ^a | FL | 4 |
| biphenyl | BP | 2 | pyrene ^a | PY | 4 |
| acenaphthylene ^a | ACL | 3 | C1-fluoranthenes/pyrenes | FP1 | 4 |
| acenaphthelene ^a | ACE | 3 | retene | Re | 4 |
| dibenzofuran | Dfu | 3 | benz[a]anthracene ^a | BaA | 4 |
| C1-naphthalenes | N1 | 2 | chrysene ^a | C0 | 4 |
| C2-naphthalenes | N2 | 2 | C1-chrysenes | C1 | 4 |
| C3-naphthalenes | N3 | 2 | C2-chrysenes | C2 | 4 |
| C4-naphthalenes | N4 | 2 | C3-chrysenes | C3 | 4 |
| fluorene ^a | F0 | 3 | C4-chrysenes | C4 | 4 |
| C1-fluorenes | F1 | 3 | benzo[b]fluoranthene ^a | BbF | 5 |
| C2-fluorenes | F2 | 3 | benzo[k]fluoranthene ^a | BkF | 5 |
| C3-fluorenes | F3 | 3 | benzo[e]pyrene | BeP | 5 |
| dibenzothiophene | D0 | 3 | benzo[a]pyrene ^a | BaP | 5 |
| C1-dibenzothiophene | D1 | 3 | perylene | Pryl | 5 |
| C2-dibenzothiophene | D2 | 3 | indeno[1,2,3-cd]pyrene ^a | IOP | 6 |
| C3-dibenzothiophene | D3 | 3 | dibenz[a,h]anthracene ^a | DA | 5 |
| anthracene ^a | AN | 3 | benzo[g,h,i]perylene ^a | BgP | 6 |
| phenanthrene ^a | P0 | 3 | coronene | Co | 6 |
| C1-phenanthrenes/anthracenes | P1 | 3 | | | |
| C2-phenanthrenes/anthracenes | P2 | 3 | | | |
| C3-phenanthrenes/anthracenes | P3 | 3 | | | |
| C4-phenanthrenes/anthracenes | P4 | 3 | | | |

^a EPA priority pollutant.

monitoring. The composition of sediment fractions was determined by stable carbon isotope analyses ($\delta^{13}\text{C}$), radio-carbon analyses ($\Delta^{14}\text{C}$), cross polarization magic angle spinning ^{13}C nuclear magnetic resonance (CPMAS ^{13}C NMR), and percent organic carbon (%TOC).

Experimental Section

Site Description and Sampling Methods. The study site is a 2–3 acre peat/clay estuary wetland at a petroleum refinery facility along the northeastern coast of the USA. Over a 20 year period, distillation waste of different gasoline blends, or pitch, was deposited into pits in the wetland. Pitch is a low volatile material similar to asphalt; during disposal, it was periodically mixed with silt, sand, and clay. The site has naturally revegetated over a 40 year period. Sediment samples were collected along a vegetation gradient over one of the pits. The pitch is ≈ 10 –15 ft in depth and is visually evident on the surface as tarlike balls. Because the area is periodically impacted by estuary tides, some sediment deposition has occurred over time. Prior analysis of surface material indicated $\approx 18\%$ total petroleum hydrocarbon contamination.

Periodic saltwater intrusion has resulted in barren areas with high salinity content (16–18 mmho/cm) that prevents plant growth; vegetated areas were moderately saline (6–7 mmho/cm). Composite sediment samples were collected in four distinct zones: (1) the barren, nonvegetated area; (2) an area of initial colonization by *Phragmites australis*; (3) an area with established stands of *Phragmites* mixed with goldenrod (*Solidago* sp. L.) and switchgrass (*Panicum* sp. L.); and (4) an area of mixed grass, tree of heaven (*Ailanthus altissima*, Desf.), and bayberry shrubs (*Myrica* sp. L.). In each zone, sediments (0–15 cm) were collected from three or four locations within a 2 m diameter area by hand trowel or shovel and mixed in a steel bowl. In vegetated areas, plants and plant litter were removed from the ground surface. Then, sediments (with roots) were collected by shovel or hand trowel in a steel bowl where roots were removed by hand and by shaking sediment free of root mass before compositing sediments. Composite sediments (≈ 2 kg) were transferred to clean plastic bags, transported on ice, and stored at 0 °C. Prior to fractionations and analyses, sediments were sieved (2 mm) to remove visual residual root material.

SOM Fractions. Sediments aliquots (10–15 g) were fractionated into water-soluble extracts, bulk sediment, bulk humin, and hydrogen fluoride/hydrogen chloride (HF/HCL) humin fractions according to previously described methods (31, 32). Replicate aliquots of fractions were analyzed for percent organic carbon (% OC) using an SOP NC 2100 CHN Analyzer (Thermo Electron S.p.A., Milan, Italy). Additional aliquots of bulk sediment, bulk humin, and HF/HCL humin were freeze-dried for 1–3 days (Benchtop 3.3/Vacu-Freeze; VirTis Co., Gardiner, NY) for isotopic analyses. Dichloromethane and methanol (DCM/MeOH) extracts were solvent exchanged under nitrogen to DCM for additional cleanup prior to GC/MS analysis.

Preferential loss of heavier alkylated PAH homologues due to the chemical fractionation of sediment was evaluated using an aliquot of Alaska north slope crude oil (ANS) that was diluted with DCM and spiked with deuterated chrysene (CHY- d_{12} , 3.5 $\mu\text{g/mL}$). Three 1-mL aliquots of fortified ANS were chemically fractionated according to the procedure described above. Initial concentrations of C3- and C4-chrysenes in the fortified ANS standard were 39 ± 1.7 and 17 ± 1.5 ng/mL, respectively. Recovered concentrations after chemical fractionation were 40 ± 6.3 and 17 ± 2.4 ng/mL, respectively. Three aliquots of soil (5 g) with no known history of PAH contamination were also amended with 1 mL of fortified ANS standard and chemically fractionated. Recovered concentrations after chemical fractionation were 40 ± 4.0 and 17 ± 1.7 ng/mL. Loss of alkylated PAHs relative to parent PAHs was not significant.

GC/MS SIM. DCM extracts of bulk sediment, bulk humin, and HF/HCL humin were first loaded onto activated neutral alumina columns prior to analysis by GC/MS. Extracts were concentrated to 5 mL and spiked with deuterated phenanthrene (d_{10} , 500 ng/mL) and benzo[a]pyrene (d_8 , 498.5 ng/mL) as internal standards. Extracts were analyzed for 42 PAHs using a modified method of EPA 8270 (33) (Table 1). GC/MS select ion monitoring (SIM) mode analyses were conducted on a HP5890 Series II GC equipped with electronic pressure control connected to an HP5970 or HP5972 MSD using a Restek 30 m \times 0.25 mm Rtx-5 (film thickness 0.25 μm) MS w/Integra-Guard column. The method is similar to that described elsewhere (34, 35).

$\delta^{13}\text{C}$ Analyses. Sediment fractions were prepared for isotope ratio mass spectrometry (IRMS) analyses by acidifying, grinding, and freeze-drying prior to submission for analyses. Stable isotope ratios of carbon were measured by continuous flow isotope ratio mass spectrometry (20–20 mass spectrometer, PDZEuropa, Northwich, UK) after sample combustion to CO_2 and N_2 at 1000 °C in an on-line elemental analyzer (PDZEuropa ANCA-GSL). Sample isotope ratios were compared to those of standard gases injected directly into the IRMS before and after the sample peaks to calculate $\delta^{15}\text{N}$ (AIR) and $\delta^{13}\text{C}$ (PDB) values. Final isotope values were adjusted to bring the mean values of standard samples distributed at intervals in each analytical run to the “true” values of the working standards. The standard for C is Pee Dee Belemnite and the standard for N is atmospheric diatomic nitrogen. Isotopic data are expressed in δ -notation, giving per mil deviation of a sample relative to a standard. Isotopic data are calculated using the equation:

$$\delta^{13}\text{C} = [({}^{13}\text{C}/{}^{12}\text{C})_{\text{sample}}/({}^{13}\text{C}/{}^{12}\text{C})_{\text{standard}} - 1] \times 1000$$

$\Delta^{14}\text{C}$ Radiocarbon Analyses. Sediment samples were sent to The National Ocean Sciences AMS facility (Woods Hole, MA) for standard radiocarbon dating analysis. Sediment fractions were combusted to CO_2 then reacted with an Fe/H_2 catalyst to form graphite. Splits of combusted samples were taken for ^{13}C analysis to correct AMS values (36). Samples were analyzed by AMS with standards (NBS Oxalic Acid I and II) (NIST-SRM-4990, 4990c) and blanks for organic carbon samples (99.9999% graphite powder, Johnson-Matthey). Data are expressed as the percent modern carbon (PMC) determined from the measurement of fraction modern that is the deviation of the $^{14}\text{C}/\text{C}$ ratio of a sample from “modern” (36).

CPMAS ^{13}C NMR. Bulk humin was treated with a 10% HF/HCl solution to reduce paramagnetic interference with ^{13}C NMR (37, 38) and then extracted with DCM. The remaining HF/HCl humin was prepared for CPMAS ^{13}C NMR analyses according to previously described methods (32). The ^{13}C NMR spectra were integrated according to the following regions: alkyl carbon (0–50 ppm); alkyl-O or C–O, C–N bonds as in alcohols, amines, carbohydrates, ethers, methoxyl and acetal carbon (50–112 ppm); aromatic carbon (112–145 ppm); phenolic carbon (145–163 ppm); carboxyl, ester, and amide C (163–190 ppm); and carbonyl carbon (190–215 ppm).

Statistical Analyses. Statistical significance was determined by Dunnett’s ANOVA ($p < 0.05$) when multiple means of vegetated data sets were compared against nonvegetated controls (40, 41). Unless otherwise noted, triplicate samples were used to determine the averaged recoveries of PAHs in sediment extracts. Values in tables represent the mean \pm one standard deviation.

Results and Discussion

For clarity, sediment samples collected from the four distinct zones in the petroleum distillate waste pit will be referred to as nonvegetated, *Phragmites* colonization, *Phragmites*/grass, and trees/shrubs sediments. For SOM fractions, the original composite samples are referred to as bulk sediment. Bulk humin represents the sediment organic matrix with humic/fulvic acids removed but the mineral matrix still intact. HF/HCl-humin represents demineralized bulk humin.

Impact of Vegetation on SOM Composition. Changes to SOM composition as vegetation colonized and developed across the waste pit are evident in CPMAS ^{13}C NMR spectra, % TOC, $\delta^{13}\text{C}$, and $\Delta^{14}\text{C}$ values (Figure 1, Table 2). *P. australis* is known to release substantial amounts of carbon via roots (42) with nearly 50% of its litter as substrate material for soils and sediments (43). SOM fractions from sediments with established stands of *Phragmites*/grass contain significantly more organic carbon than nonvegetated SOM fractions (Table

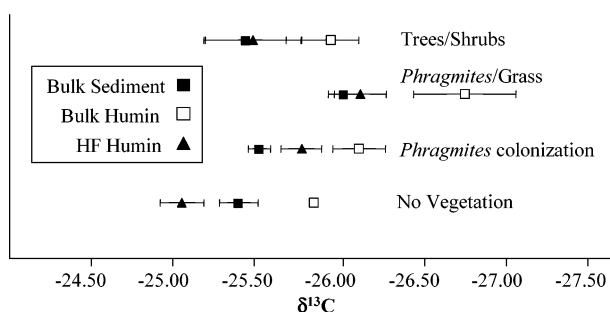


FIGURE 1. $\delta^{13}\text{C}$ values for bulk sediment, bulk humin, and HF/HCl humin fractions of sediment from nonvegetated and vegetated areas at a petroleum distillate waste pit. Values represent mean \pm one standard deviation ($n = 3$). Error bars for bulk humin, nonvegetated are smaller than the box marker.

TABLE 2. Means of the Sum of Alkylated and Non-Alkylated PAHs Concentrations (WTPAH),^b the Sum of 16 Priority PAHs,^b the Percent Organic Carbon (TOC), and the Percent Modern Carbon (PMC)^c for Fractions of Refinery Waste Pit Sediment^a

| | non-vegetated | <i>Phragmites</i> colonization | <i>Phragmites</i> mixed grass | trees, shrubs, and grass |
|----------------------|----------------|--------------------------------|-------------------------------|--------------------------|
| Bulk Sediment | | | | |
| %TOC | 21 \pm 1.9 | 18 \pm 0.14 | 27 \pm 0.37 | 21 \pm 1.6 |
| ^{14}C PMC | 2.0 \pm 0.06 | N/A ^d | 24 \pm 0.16 | N/A |
| [TPAH] (mg/g soil) | 161 \pm 11.8 | 110 \pm 11.6 | 69 \pm 2.9 | 62 \pm 1.4 |
| 16 PAH (mg/g soil) | 34 \pm 4.9 | 29 \pm 2.4 | 19 \pm 2.0 | 18 \pm 0.63 |
| [TPAH] (mg/g OC) | 767 \pm 125 | 611 \pm 67.8 | 254 \pm 14.4 | 293 \pm 28.9 |
| Bulk Humin | | | | |
| %TOC | 7.5 \pm 0.22 | 12 \pm 0.82 | 13 \pm 0.11 | 11 \pm 0.56 |
| ^{14}C PMC | 6.1 \pm 0.14 | N/A | 44 \pm 0.3 | N/A |
| [TPAH] (mg/g soil) | 14 \pm 1.9 | 11 \pm 2.1 | 11 \pm 1.2 | 8.4 \pm 0.45 |
| 16 PAH (mg/g soil) | 3.8 \pm 1.00 | 3.4 \pm 0.75 | 3.0 \pm 0.30 | 3.3 \pm 0.79 |
| [TPAH] (mg/g OC) | 181 \pm 29.3 | 90 \pm 23 | 81 \pm 9.5 | 76 \pm 8.7 |
| HF/HCl Humin | | | | |
| %TOC | 10 \pm 1.8 | 12 \pm 2.0 | 28 \pm 0.98 | 35 \pm 1.6 |
| ^{14}C PMC | 2.1 \pm 0.08 | N/A | 33 \pm 0.20 | N/A |
| [TPAH] (mg/g soil) | 6.0 \pm 1.0 | 3.1 \pm 0.27 | 2.8 \pm 0.27 | 3.6 \pm 0.81 |
| 16 PAH (mg/g soil) | 1.1 \pm 0.50 | 0.7 \pm 0.10 | 0.5 \pm 0.15 | 1.2 \pm 0.68 |
| [TPAH] (mg/g OC) | 60 \pm 21 | 26 \pm 6.8 | 10 \pm 1.4 | 10 \pm 2.7 |

^a Values are means \pm one standard deviation ($n = 3$). ^b See Table 1. ^c Analyses conducted by NOAA/WHOI AMS facility. ^d N/A = not analyzed.

2, Dunnett’s ANOVA, $p < 0.05$). Humin fractions from trees/shrubs sediments also contain significantly more organic carbon than nonvegetated SOM fractions (Table 2, Dunnett’s ANOVA, $p < 0.05$).

SOM reflects the photosynthetic pathway of dominant plant species, and terrestrial plants are classified isotopically by two categories of CO_2 fixation, the Calvin cycle (C_3 , $^{13}\text{C}/^{12}\text{C} \approx -27\text{‰}$) and the Hatch–Slack cycle (C_4 , $^{13}\text{C}/^{12}\text{C} \approx -12\text{‰}$). $\delta^{13}\text{C}$ values indicate that increased organic carbon content in vegetated SOM fractions reflects inputs of biogenic carbon from vegetation as SOM isotopic signatures shift toward the biogenic source (Figure 1, Table 2). *Phragmites*, a C_3 plant, represents modern, biogenic carbon with more negative carbon isotope signatures ($^{13}\text{C}/^{12}\text{C} \approx -26.4\text{‰}$) (44, 45) than petroleum distillate waste ($^{13}\text{C}/^{12}\text{C} \approx -25\text{‰}$). The addition of *Phragmites* carbon to petroleum distillate waste should negatively shift isotopic signatures. In Figure 1, $\delta^{13}\text{C}$ values for fractions from *Phragmites*/grass were significantly more negative than other SOM fractions (Dunnett’s ANOVA, $p < 0.05$). These isotopic shifts contradict expected $\delta^{13}\text{C}$ fractionation patterns if PAH biodegradation is present due to isotopic effects. Kinetic isotopic effects often result in preferential microbial degradation of ^{12}C relative to ^{13}C . Thus,

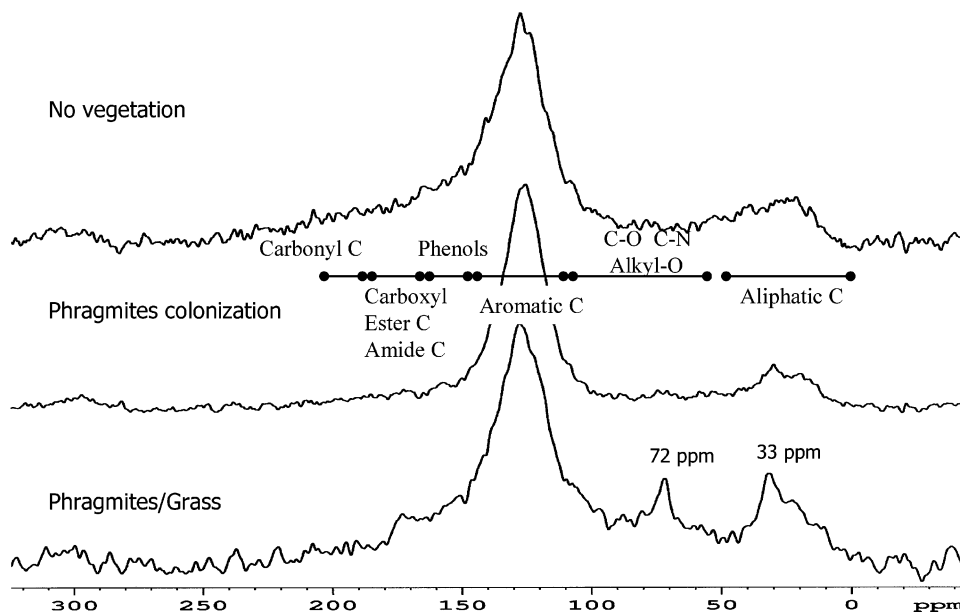


FIGURE 2. Cross-polarization magic angle spinning (CPMAS) ^{13}C nuclear magnetic resonance spectra of HF/HCl humin fractions for nonvegetated, *Phragmites* colonization, and *Phragmites* with mixed grass areas.

remaining parent material in SOM such as PAHs, cellulose, and hemicellulose are 1–2‰ more positive than original parent PAHs, and biodegraded residues such as lignin and PAH metabolites are –2 to –6‰ more negative (46). $\delta^{13}\text{C}$ values for SOM become more negative as vegetation is established; however, fractionation is not uniform for all PAHs, and for complex matrixes such as petroleum distillate wastes, fractionation may be obscured in bulk carbon isotope analyses.

Prior studies have shown that $\delta^{13}\text{C}$ values for humin are typically more positive than bulk soil, but when a different carbon source is introduced to SOM, $\delta^{13}\text{C}$ values for bulk sediment and humin become similar to one another (47). For nonvegetated sediments, $\delta^{13}\text{C}$ values for humin are more positive than bulk soil. For established vegetated sediments (*Phragmites*/grass and trees/shrubs), $\delta^{13}\text{C}$ values for bulk sediment and humin are not significantly different (Dunnnett's ANOVA, $p < 0.05$). These results indicate the input of a different carbon source to SOM fractions in vegetated sediments.

The C content of petroleum contains very little ^{14}C activity because of its ancient origin; whereas, modern plant carbon and recent humification of modern plant carbon will reflect modern ^{14}C activity from atmospheric $^{14}\text{CO}_2$. Radiocarbon ^{14}C analyses for SOM fractions from nonvegetated sediments and *Phragmites*/grass (Table 2) confirm that increased organic carbon content in vegetated SOM fractions reflects inputs of modern plant carbon when compared to ^{14}C values for nonvegetated SOM fractions (Table 2). The ^{14}C content of nonvegetated SOM fractions ranged from 2 to 6% modern carbon, while ^{14}C content of *Phragmites*/grass contained 24–44% modern carbon (Table 2). The ^{14}C content of petroleum carbon and C3-derived plant/soil C are much more dissimilar than $\delta^{13}\text{C}$ signatures, which allows for easier differentiation of carbon sources.

The impact of modern plant carbon on HF/HCl humin carbon composition is evident in Figure 2. CPMAS ^{13}C NMR spectra for HF/HCl humin fractions for three of the four areas are shown; the CPMAS ^{13}C NMR spectrum for trees/shrubs areas is not shown due to paramagnetic interferences during spectrum acquisition, even after extensive HF/HCl digestion. All spectra exhibit aromatic C (112–145 ppm) and phenolic (145–163 ppm) structures that are expected for an asphaltlike matrix.

The CPMAS ^{13}C NMR spectrum for *Phragmites*/grass exhibits new, major shifts at 33 ppm (aliphatic C; methylene carbons) and 72 ppm (O-alkyl C; carbohydrate carbons). Paraffinic carbons (0–50 ppm), such as plant-derived biopolymers (33 ppm), are preserved in humin fractions relative to more labile carbon materials, such as fatty acids, proteins, and polysaccharides (48); lignins, tannins, and aromatic carbon can also be preserved (39, 49). Other signature shifts for refractory plant-derived organic matter include 55 and 150 ppm for lignin; 21 ppm for esterified hemicellulose; 72 ppm for C₂-, C₃-, C₅-cellulose and -hemicellulose; 64, 84, 105 for C₆, C₄, C₁, respectively, for carbohydrates and polysaccharides; and 172 ppm for carbohydrate residues (39, 50, 51). Except for the major shift at 72 ppm, these shifts are not discernible and would suggest that residual lignin and carbohydrate residues are not present. On the basis of %TOC and stable isotope analyses of HF/HCl humin for *Phragmites*/grass, the shift at 33 ppm most likely represents aliphatic C from *Phragmites*.

Previous work has identified chemical shifts for pyrene *cis*-4,5-dihydrodiol (71.9 and 127 ppm) and mono and dihydroxylated pyrene metabolites extracted from humic fractions of [4,9- $^{13}\text{C}_2$]pyrene-amended sediments (32). Similar chemical shifts could be expected for other hydroxylated PAHs and PAH dihydrodiols in petroleum distillate waste. The absence of other expected shifts for carbohydrates and polysaccharides noted above indicate that the chemical shift at 72 ppm reflects the presence of PAH metabolites sequestered in HF/HCl humin from *Phragmites*/grass areas. Aliphatic carbon persists in SOM, humin, and kerogen and is preserved through humification processes (39, 49); aliphatic carbon can also sorb PAHs significantly (51, 52). Thus, plant-derived aliphatic carbon could sorb PAHs and hydroxylated or dihydrodiol PAH intermediates from the distillate waste matrix and sequester them in humin (31, 32).

Collectively, %TOC, $\delta^{13}\text{C}$, $\Delta^{14}\text{C}$, and ^{13}C NMR analyses demonstrate modern plant carbon inputs from *Phragmites* to sediment fractions and suggest that plant-derived aliphatic carbon appears to be preserved in humin fractions. The slow turnover of aliphatic carbon in SOM, particularly in humin fractions (48), and ^{13}C NMR data suggests that aliphatic carbon can play a major role in sorbing PAHs and PAH metabolites in vegetated SOM fractions. Alternatively, aliphatic carbon could enhance refractory PAH bioaccessibility

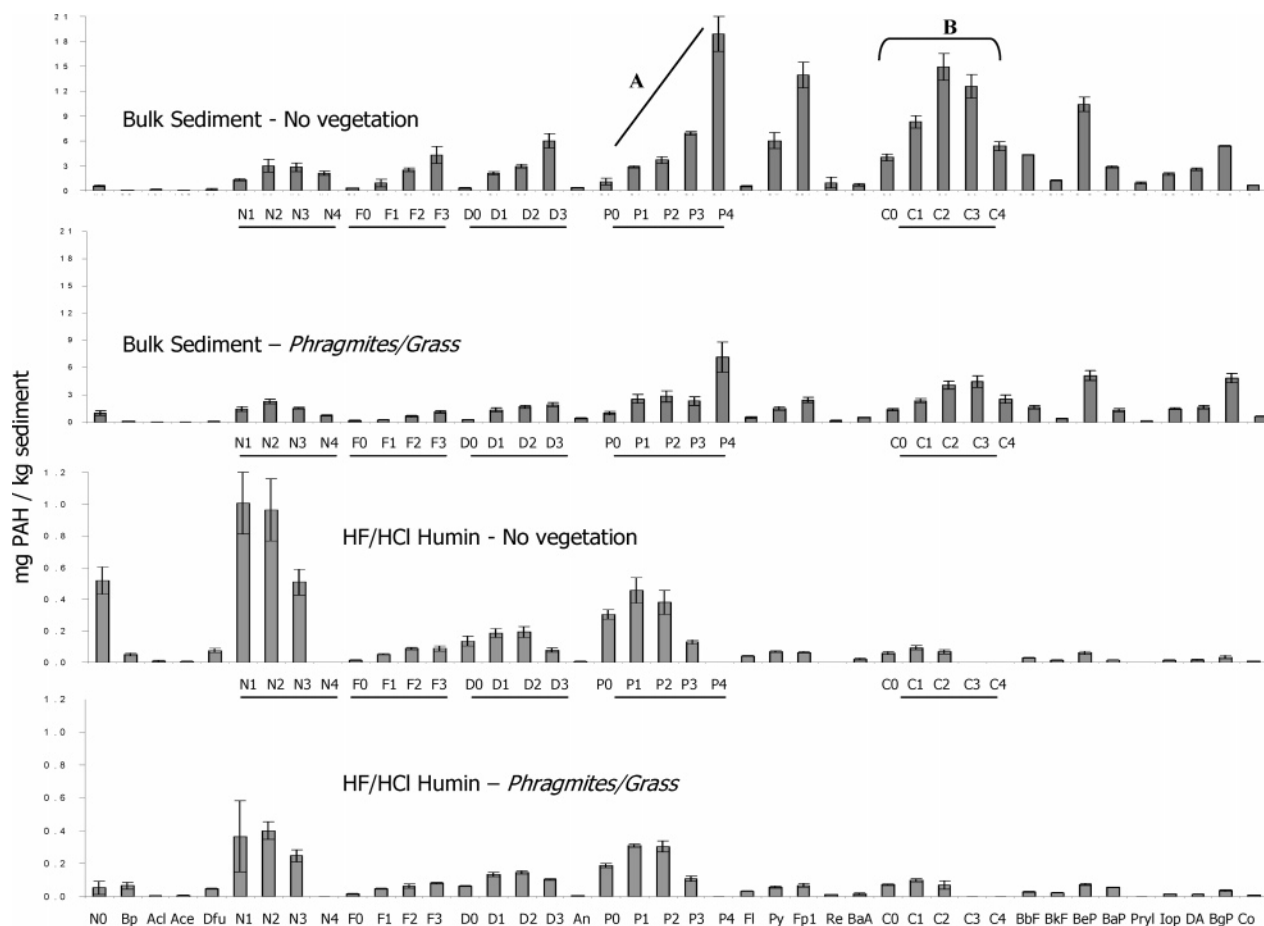


FIGURE 3. PAH histograms for selected sediment fractions of nonvegetated and vegetated sites. Concentrations are in mg of PAH/kg of sample material. A indicates patterns for nonweathered distribution patterns and B indicates patterns for weathered distribution patterns. Error bars are mean \pm one standard deviation ($n = 3$ or $n = 4$). For peak ID, see Table 1.

by partitioning PAHs from the petroleum distillate waste matrix. Perhaps, PAH metabolites present in HF/HCl humin are the result of degraded PAHs desorbed by aliphatic plant carbon.

If plant organic matter, particularly aliphatic plant carbon, improves PAH bioaccessibility and PAH transformation, then PAH concentrations in vegetated SOM fractions should be significantly lower than PAH concentrations in nonvegetated SOM fractions. Also, distribution patterns in PAH histograms and PAH compound ratios should be more weathered for vegetated SOM fractions than nonvegetated SOM fractions. If plant organic matter retards PAH bioaccessibility, then significant declines in PAH concentrations normalized to organic carbon content and weathered diagnostic indices should not be observed.

PAH Concentrations, Distribution Patterns, and Compound Ratios. Mean concentrations of 42 alkylated and nonalkylated PAHs ([TPAH]) declined significantly (Dunnett's ANOVA, $p < 0.05$) from nonvegetated areas to vegetated areas for bulk sediment and HF/HCl humin fractions (Table 2). For the 16 priority PAHs (Table 1), significant PAH concentration declines were only apparent for bulk sediment fractions (Dunnett's ANOVA, $p < 0.05$). For bulk humin fractions, mean [TPAH] were significantly lower only in trees/shrubs bulk humin.

To account for lower [TPAH] recovery due to carbon dilution from plant carbon inputs, [TPAH] were carbon-normalized for each SOM fraction (Table 2). Declines in [TPAH] are more apparent for all vegetated SOM fractions, particularly for vegetated humin. Without carbon normalization, percent losses of [TPAH] from nonvegetated fractions

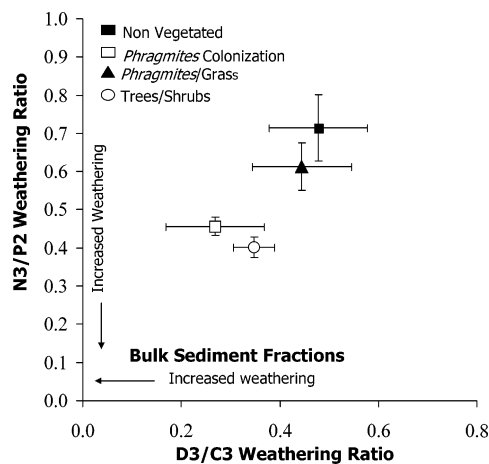


FIGURE 4. Double-ratio plots of two weathering ratios, C3-naphthalenes and C2-phenanthrenes (N3/P2) and C3-dibenzothiophenes to C3-chrysenes (D3/C3), for bulk sediment fractions from nonvegetated and vegetated areas at a petroleum distillate waste pit. Values represent mean \pm one standard deviation ($n = 3$).

to established vegetated SOM fractions are similar for bulk sediment (57%) and humin (53%). When [TPAH] are carbon normalized to %TOC in SOM fractions, percent losses of [TPAH] from nonvegetated fractions to established vegetated SOM fractions are greater in humin (83%) than bulk sediment (67%). These results suggest that PAH transformation, as measured by [TPAH] loss, is as extensive in vegetated humin as bulk sediment.

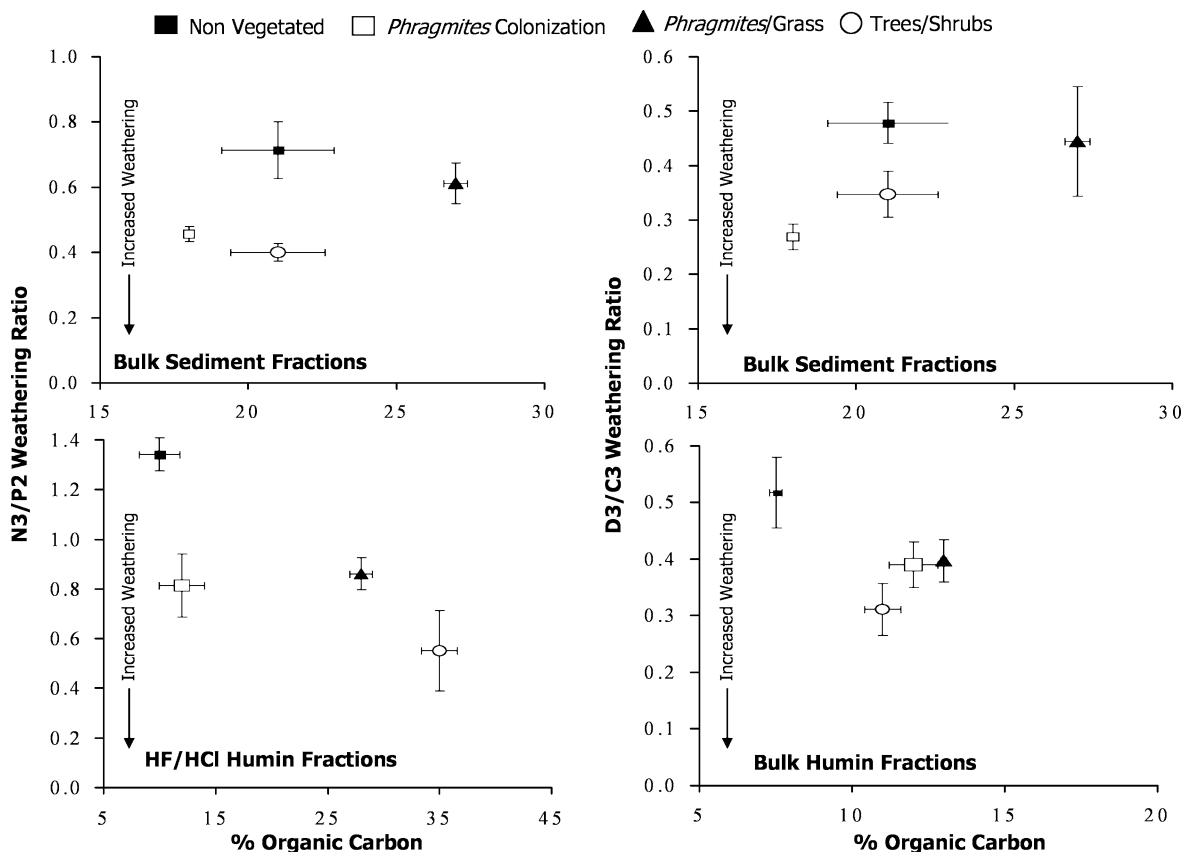


FIGURE 5. Ratio plots of two weathering ratios, C3-naphthalenes and C2-phenanthrenes (N3/P2) and C3-dibenzothiophenes to C3-chrysenes (D3/C3), to %TOC for SOM fractions from nonvegetated and vegetated areas at a petroleum distillate waste pit. Values represent mean \pm one standard deviation ($n = 3$).

Figure 3 shows PAH distributions for bulk sediment and HF/HCl humin fractions from nonvegetated and *Phragmites*/grass sediments (Figure 3). Distributions of parent (non-alkylated) and alkylated PAHs can distinguish between PAH sources such as petroleum, creosote, or urban soot (53). For each particular source (pyrogenic vs petrogenic), distributions of PAHs can *qualitatively* indicate if weathering has occurred. For mixed source sites, interpretation of weathering can be more problematic. For this site, a primarily petrogenic source, distributions of nonweathered PAHs should appear bell-shaped for alkylated families such as naphthalenes (N0–N4), phenanthrenes/anthracenes (P0–P4), dibenzothiophenes (D0–D3), fluoranthenes/pyrene (F0–F3), and chrysenes (C0–C4). Petrogenic sources contain more alkylated PAHs at greater concentrations than parent or nonalkylated PAHs (53). Because alkylated PAHs “weather” more slowly than parent PAHs, weathered petrogenic histograms are skewed for each homologue series along a pattern of increased abundance with increased alkylation (34). Biodegradation is often the primary mechanism for PAH weathering, but volatilization and leaching may also weather the lighter PAHs as plants physically disturb the petroleum distillate matrix (29).

In Figure 3, weathered PAH distribution patterns (A) are apparent for fluorene, dibenzothiophenes, and phenanthrene homologues in bulk sediment fractions and are not apparent for chrysene homologues (B). In all HF/HCl humin fractions, naphthalene, phenanthrene, and their alkylated homologues are present at greater concentrations than other PAHs. Increased concentrations of these PAHs may indicate their ability, as smaller molecular weight PAHs, to diffuse faster and with less steric hindrance into humin matrixes (54, 55). For HF/HCl humin fractions, fluorene homologues indicate weathering. Steric hindrance may also play a role in obscuring

dibenzothiophene and phenanthrene weathering patterns because more alkylated homologues are less likely to be present in humin (54, 55).

Compound ratios provide a more quantitative measure of PAH weathering and can be used to quantify the degree of weathering and biodegradation of spilled oil and to predict and monitor the effectiveness of remediation activities (53, 56). The ratio of C3-naphthalenes and C2-phenanthrenes (N3/P2) can be used for diesel fuel and crude oil in the early stages of weathering, while the ratio of C3-dibenzothiophenes to C3-chrysenes (D3/C3) can be used in later stages of weathering (56). D3/C3 ratios could not be determined for humin fractions due to the absence of C3-chrysenes. The absence of C3-chrysene is not attributable to our fractionation methodology, as discussed earlier in the Experimental Section, but is most likely due to steric interactions that impede diffusion into refractory humin.

In Figure 4, a cross plot of N3/P2 to D3/C3 weathering ratios shows that bulk sediments from *Phragmites* colonization and trees/shrubs areas are more weathered than bulk sediment fractions from nonvegetated and *Phragmites*/grass areas. Weathering for bulk sediments from *Phragmites* colonization and trees/shrubs areas does not correlate with %TOC, as shown in Figure 5. However, there does appear to be a relationship between N3/P2 weathering ratios and %TOC for humin fractions (Figure 5). Vegetated humin fractions are more weathered than nonvegetated humin, and these fractions contain more plant carbon, as isotopic and radio-carbon analyses indicate.

We postulated two mechanisms by which plant-derived organic matter might influence PAH fate in vegetative systems. Plant organic matter may improve PAH bioaccessibility by destabilizing SOM and liberating PAHs for transformation; alternatively, plant organic matter may provide

new carbon matrixes that sorb and bind PAHs. Presented data ($\delta^{13}\text{C}$, %TOC, $\Delta^{14}\text{C}$, and CPMAS ^{13}C NMR) show the presence of new plant carbon in SOM fractions, particularly humin fractions, from established vegetated areas. A relationship between declines in [TPAH], PAH weathering ratios, and inputs of biogenic carbon is apparent for vegetated SOM fractions. Observed PAH metabolites sequestered in *Phragmites*/grass humin are related to inputs of biogenic carbon, but whether sequestered metabolites are associated with aliphatic plant carbon or the residual asphaltlike matrix cannot be determined by the presented ^{13}C NMR data. Reductions of [TPAH] and inputs of biogenic carbon were as great if not greater in vegetated humin fractions as in vegetated bulk sediments. Collectively, these results show that plant organic matter does impact PAH transformation and bioaccessibility in both labile and refractory fractions of petroleum distillate waste.

Acknowledgments

We would like to thank Dr. Evelyn Drake, Dr. David Harris, and Dr. Patrick Hatcher for their assistance with sample collection, data analysis, and manuscript review. We also thank the reviewers for their suggestions and comments to improve the manuscript. Radiocarbon analyses were provided by the National Ocean Sciences AMS facility and NSF (OCE-9807266). This work was supported with research funding from The National Science Foundation CHE-0089147 and BES-0337453.

Literature Cited

- Seiple, K.; Doick, K.; Jones, K.; Burauel, P.; Craven, A.; Harms, H. Defining bioavailability and bioaccessibility of contaminated soil and sediment is complicated. *Environ. Sci. Technol.* **2004**, *38*, 229–231.
- Burdon, J. Are the traditional concepts of the structures of humic substances realistic. *Soil Sci.* **2001**, *166*, 752–769.
- Golchin, A.; Clarke, P.; Baldock, J.; Higashi, T.; Skjemstad, J.; Oades, J. The effects of vegetation and burning on the chemical composition of soil organic matter in a volcanic ash soil as shown by ^{13}C NMR spectroscopy. I. Whole soil and humic acid fraction. *Geoderma* **1997**, *76*, 155–174.
- Piccolo, A. The supramolecular structure of humic substances. *Soil Sci.* **2001**, *166*, 810–832.
- Hedges, J. I.; Oades, J. M. Comparative organic geochemistries of soils and marine sediments. *Org. Geochem.* **1997**, *27*, 319–361.
- Spaccini, R.; Piccolo, A.; Conte, P.; Haberhauer, G.; Gerzabek, M. Increased soil organic carbon sequestration through hydrophobic protection by humic substances. *Soil Biol. Biochem.* **2002**, *34*, 1839–1851.
- Kamath, R.; Schnoor, J. L.; Alvarez, P. J. Effect of root-derived substrates on the expression of *nah-lux* genes in *Pseudomonas fluorescens* HK44: Implications for PAH biodegradation in the rhizosphere. *Environ. Sci. Technol.* **2004**, *38*, 1740–1745.
- Binet, P.; Portal, J.; Leyval, C. Dissipation of 3–6 ring polycyclic aromatic hydrocarbons in the rhizosphere of ryegrass. *Soil Biol. Biochem.* **2000**, *32*, 2011–2017.
- Joner, E.; Corgie, S.; Amellal, N.; Leyval, C. Nutritional constraints to degradation of polycyclic aromatic hydrocarbons in a simulated rhizosphere. *Soil Biol. Biochem.* **2002**, *34*, 859–864.
- Chen, U. C.; Banks, M. K.; Schwab, A. P. Pyrene degradation in the rhizosphere of tall fescue (*Festuca arundinacea*) and switchgrass (*Panicum virgatum* L.). *Environ. Sci. Technol.* **2003**, *37*, 5778–5782.
- Armstrong, J.; Armstrong, W. An overview of the effects of phytotoxins on *Phragmites australis* in relation to die-back. *Aquat. Bot.* **2001**, *69*, 251–268.
- Conte, P.; Zena, A.; Pilidis, G.; Piccolo, A. Increased retention of polycyclic aromatic hydrocarbons in soils induced by soil treatment with humic substances. *Environ. Pollut.* **2001**, *112*, 27–31.
- Cozzolino, A.; Conte, P.; Piccolo, A. Conformational changes of humic substances induced by some hydroxy-, keto-, and sulfonic acids. *Soil Biol. Biochem.* **2001**, *33*, 563–571.
- Nardi, S.; Reniero, F.; Concheri, G. Soil organic matter mobilization by root exudates of three maize hybrids. *Chemosphere* **1997**, *35*, 2237–2244.
- Piccolo, A.; Conte, P.; Trivellone, E.; Van Lagen, B.; Buurman, P. Reduced heterogeneity of a lignite humic acid by preparation HPSEC following interaction with an organic acid. Characterization of size-separates by Pyr–GC–MS and ^1H NMR Spectroscopy. *Environ. Sci. Technol.* **2002**, *36*, 76–84.
- Kopinke, F. D.; Georgi, A.; Mackenzie, K. Sorption of pyrene to dissolved humic substances and related model polymers. I. Structure–property correlation. *Environ. Sci. Technol.* **2001**, *35*, 2536–2542.
- Perminova, I. V.; Grechishcheva, Y. N.; Kovalevskii, D. V.; Kudryavtsev, A. V.; Petrosyan, V. S.; Matorin, D. N. Quantification and prediction of the detoxifying properties of humic substances related to their chemical binding to polycyclic aromatic hydrocarbons. *Environ. Sci. Technol.* **2001**, *35*, 3841–3848.
- Ressler, B. P.; Kneifel, H.; Winter, J. Bioavailability of polycyclic aromatic hydrocarbons and formation of humic acid-like residues during bacterial PAH degradation. *Appl Microbiol. Biotechnol.* **1999**, *53*, 85–91.
- Holman, H.; Nieman, K.; Sorensen, D.; Miller, C.; Martin, M.; Borch, T.; McKinney, W.; Sims, R. Catalysis of PAH biodegradation by humic acid shown in synchrotron infrared studies. *Environ. Sci. Technol.* **2002**, *36*, 1276–1280.
- Huang, Q.; Selic, H.; Weber, W. Peroxidase-catalyzed oxidative coupling of phenols in the presence of geosorbents: Rates of nonextractable product formation. *Environ. Sci. Technol.* **2002**, *36*, 596–602.
- Piccolo, A.; Cozzolino, A.; Conte, P.; Spaccini, R. Polymerization by enzyme-catalyzed oxidative couplings of supramolecular associations of humic molecules. *Naturewissenschaften* **2000**, *87*, 391–394.
- Liste, H.-H.; Alexander, M. Accumulation of phenanthrene and pyrene in rhizosphere soil. *Chemosphere* **2000**, *40*, 11–14.
- White, J. C.; Kottler, B. Citrate-mediated increase in the uptake of weathered 2,2-Bis(p-chlorophenyl)1,1-dichloroethylene residues by plants. *Environ. Toxicol. Chem.* **2002**, *21*, 550–556.
- Cardon, Z.; Hungate, B.; Cambardella, C.; Chapin, F.; Field, C.; Holland, E.; Mooney, H. Contrasting effects of elevated CO_2 on old and new soil carbon pools. *Soil Biol. Biochem.* **2001**, *33*, 365–373.
- Hungate, B.; Holland, E.; Jackson, R.; Chapin, F.; Mooney, H.; Field, C. The fate of carbon in grasslands under carbon dioxide enrichment. *Nature* **1997**, *388*, 576–579.
- Schlesinger, W.; Lichter, J. Limited carbon storage in soil and litter of experimental forest plots under increased atmospheric CO_2 . *Nature* **2001**, *411*, 466–468.
- Yang, Y.; Ratte, D.; Smets, B.; Pignatello, J.; Grasso, D. Mobilization of soil organic matter by complexing agents and implications for polycyclic aromatic hydrocarbon desorption. *Chemosphere* **2001**, *43*, 1013–1021.
- Talley, J.; Ghosh, U.; Tucker, S.; Furey, J.; Luthy, R. Particle-scale understanding of the bioavailability of PAHs in sediment. *Environ. Sci. Technol.* **2002**, *36*, 477–483.
- Widdowson, M. A.; Shearer, S.; Anderson, R. G.; Novak, J. T. Remediation of polycyclic aromatic hydrocarbon compounds in groundwater using poplar trees. *Environ. Sci. Technol.* **2005**, *39*, 1598–1605.
- Olson, P.; Fletcher, J. Field evaluation of mulberry root structure with regard to phytoremediation. *Bioremediat. J.* **1999**, *3*, 27–33.
- Guthrie, E. A.; Bortiatynski, J. M.; Van Heemst, J. D. H.; Richman, J. E.; Hardy, K. S.; Kovach, E. M.; Hatcher, P. G. Determination of [^{13}C]pyrene sequestration in sediment microcosms using flash pyrolysis–GC–MS and ^{13}C NMR. *Environ. Sci. Technol.* **1999**, *33*, 119–125.
- Guthrie-Nichols, E. A.; Grasham, A.; Kazunga, C.; Salloom, M.; Sangaiah, R.; Gold, A.; Hatcher, P. G. The effect of aging on pyrene transformation in sediments. *Environ. Toxicol. Chem.* **2003**, *22*, 40–49.
- Environmental Protection Agency. *SW-846 Manual for Waste Testing*; EPA, Washington, DC, 1986; Volumes 1B and 1C.
- Stout, S. A.; Uhler, A. D.; McCarthy, K. J.; Emsbo-Mattingly, S. D. In *Introduction to Environmental Forensics*; Murphy, B. L., Morrison, R. D., Eds.; Academic Press: San Diego, CA, 2002; pp 137–260.
- Luellen, D.; Shea, D. Calibration and Field Verification of Semipermeable Membrane Devices for Measuring Polycyclic Aromatic Hydrocarbons in Water. *Environ. Sci. Technol.* **2002**, *36*, 1791–1797.

- (36) Stuiver, M.; Polach, H. A. Discussion: Reporting of ^{14}C data. *Radiocarbon* **1977**, *19*, 355–363.
- (37) Cook, R.; Langford, C.; Yamdagni, R.; Preston, C. A modified cross-polarization magic angle spinning ^{13}C NMR procedure for the study of humic materials. *Anal. Chem.* **1996**, *68*, 3979–3986.
- (38) Gelinas, Y.; Baldock, J. A.; Hedges, J. I. Demineralization of marine and freshwater sediments for CP/MAS ^{13}C NMR analysis. *Org. Geochem.* **2001**, *32*, 677–693.
- (39) Hatcher, P. G.; Breger, I. A.; Dennis, L. W.; Maciel, G. E. Solid-state carbon- ^{13}C -NMR of sedimentary humic substances: New revelations on their chemical composition. In *Aquatic and Terrestrial Humic Materials*; Christman, R., Gjessing, E., Eds.; Ann Arbor Science: Ann Arbor, MI, 1983; pp. 37–82.
- (40) Dunnett, C. W. A multiple comparison procedure for comparing several treatments with a control. *J. Am. Stat. Assoc.* **1955**, *272*, 1096–1121.
- (41) Dunnett, C. W. New tables for multiple comparisons with a control. *Biometrics* **1964**, *20*, 482–491.
- (42) Minchinton, T. Disturbance by wrack facilitates spread of *Phragmites australis* in a coastal marsh. *J. Exp. Mar. Biol. Ecol.* **2002**, *281*, 89–107.
- (43) Asaeda, T.; Nam, L.; Hietz, P.; Tanaka, N.; Karunaratne, S. Seasonal fluctuations in live and dead biomass of *Phragmites australis* as described by a growth and decomposition model: Implications of duration of aerobic conditions for litter mineralization and sedimentation. *Aquat. Bot.* **2002**, *73*, 223–239.
- (44) Antonielli, M.; Pasqualini, S.; Batini, P.; Ederlie, L.; Massacci, A.; Loreto, F. Physiological and anatomical characterization of *Phragmites australis* leaves. *Aquat. Bot.* **2002**, *72*, 55–66.
- (45) Cloern, J.; Canuel, E.; Harris, D. Stable carbon and nitrogen isotope composition of aquatic and terrestrial plants of the San Francisco Bay estuarine system. *Limnol. Oceanogr.* **2002**, *47*, 713–729.
- (46) Yanik, P.; O'Donnell, T.; Macko, S.; Qian, Y.; Kennicutt, M. The Isotopic Compositions of Selected Crude Oil PAHs During Biodegradation. *Org. Geochem.* **2003**, *34*, 291–304.
- (47) Lichtfouse, E.; Dou, S.; Houot, S.; Barriuso, E. Isotope evidence for soil organic carbon pools with distinct turnover rates-II. Humic substances. *Org. Geochem.* **1995**, *23*, 845–847.
- (48) Lichtfouse, E. Temporal Pools of Individual Organic Substances in Soil. *Analysis* **1999**, *27*, 442–444.
- (49) Rice, J. Humins. *Soil Sci.* **2001**, *166*, 848–857.
- (50) Gunasekara, A. S.; Simpson, M. J.; Xing, B. Identification and Characterization of Sorption Domains in Soil Organic Matter Using Structurally Modified Humic Acids. *Environ. Sci. Technol.* **2003**, *37*, 852–858.
- (51) Chefetz, B.; Deshmukh, A. P.; Hatcher, P. G.; Guthrie, E. A. Pyrene sorption by natural organic matter. *Environ. Sci. Technol.* **2000**, *34*, 2925–2930.
- (52) Salloum, M.; Chefetz, B.; Hatcher, P. G. Phenanthrene sorption by aliphatic-rich natural organic matter. *Environ. Sci. Technol.* **2002**, *36*, 1953–1958.
- (53) Stout, S. A.; Uhler, A. D.; Emsbo-Mattingly, S. D. Comparative Evaluation of Background Anthropogenic Hydrocarbons in Surficial Sediments from Nine Urban Waterways. *Environ. Sci. Technol.* **2004**, *38*, 2987–2994.
- (54) Shor, L.; Rockne, K.; Taghon, G.; Young, L.; Kosson, D. Desorption kinetics for field-aged polycyclic aromatic hydrocarbons from sediments. *Environ. Sci. Technol.* **2003**, *37*, 1535–1544.
- (55) van Noort, P. C. M.; Corneilissen, G.; ten Hulscher, T. E. M.; Vrind, B. A.; Rigterink, H.; Belfroid, A. Slow and very slow desorption of organic compounds from sediment; influence of sorbate polarity. *Water Res.* **2003**, *37*, 2317–2322.
- (56) Douglass, G. S.; Bence, A. E.; Prince, R. C.; McMillen, S. J.; Butler, E. L. Environmental stability of selected petroleum hydrocarbon source and weathering ratios. *Environ. Sci. Technol.* **1996**, *30*, 2332–2339.

Received for review December 13, 2004. Revised manuscript received April 15, 2005. Accepted May 10, 2005.

ES048028O